Radiation Physics and Chemistry 190 (2022) 109816

Contents lists available at ScienceDirect

Radiation Physics and Chemistry

journal homepage: www.elsevier.com/locate/radphyschem

The Monte Carlo simulation approach to verification of the attenuation factors *k* for isotropic gamma-ray sources commonly used in industry, medicine and science

Marta Błażkiewicz, Adam Konefał *

Institute of Physics, University of Silesia in Katowice, Katowice, Poland

ARTICLE INFO

Keywords:
Attenuation factors
Gamma rays
Isotropic radiation sources
Monte Carlo simulation
Radiological protection
Protective materials

ABSTRACT

An important problem, which is currently overlooked in radiological protection, is the omission of the contribution from low-energy photons when estimating the dose received by persons working in conditions of exposure to ionizing radiation. As shown in this study, this contribution cannot be omitted because it determines the dose in the workplace when an isotropic source of gamma rays (uncollimated beams) and thick shields are used. The omission of the contribution from low-energy photons causes that the gamma-ray attenuation factors, often marked in radiological protection with the letter *k*, as well as the transmission curves for isotropic gamma-ray beams resemble those for collimated beams without the typical features of uncollimated beams. This causes the estimated doses to be significantly underestimated. In this work the gamma-ray attenuation factors *k* were determined by Monte Carlo simulations for basic shielding materials, for commonly used isotropic gamma-ray sources. These factors are the basic parameters used to calculate the gamma-ray dose that a person who performs professional activities with gamma rays can receive. Accurate calculation of this dose translates into work safety. Justification for this research is the necessity to apply the exact *k*-factor values in radiological protection in Poland where doses at workplaces are calculated according to the procedure given in Gostkowska's book based on the old Polish norm (1987). The ground of this norm are transmission curves from NCRP Report 49 (1976) based on data obtained in the 1930's, 40's and 50's, unsuitable for isotropic sources. Although the obtained results refer to the Polish standard, the world's norms based on the NCRP Report 49 also need innovation, because the subsequent versions of this report published in 1991, 1994 and 1998 as well as the NCRP Report No. 151 considered as the new face of the NCRP Report No. 49 do not make the required correction. This work meets these requirements by using the Monte Carlo simulation method based on the GEANT4 code.

1. Introduction

In the last decade the use of radiation sources spread over various branches of human activity. Presently the radiation sources are applied in industry, medicine and science. The primary device used to monitor the dose or dose rate in the workplace is the radiometer. There are currently three types of radiometers in use. One type of these devices is equipped with one or more Geiger-Müller counters. The second type uses semiconductors. Less commonly, radiometers are based on scintillation detectors. However, in most cases, the measurement threshold of all types of radiometers for gamma radiation is 100 keV or greater. As a result, the measurement of the dose or the dose rate with the use of a radiometer eliminates the contribution from low-energy photons originating from the scattering of higher-energetic gamma rays or from de-excitation of excited or ionized atoms of the radiation shield. As this study proves, the contribution from low-energy photons dominates in the case of isotropic gamma-ray sources when thick shields are used. Currently, this contribution is not taken into account in radiological protection, not only because the design of typical radiometers does not allow it, but also because the current norms and standards do not provide the necessary data. The use of the radiation sources is regulated by the Nuclear Law. In this work the discussed problem was examined for standards in force in radiological protection in Poland. The Polish Nuclear Law (2003) is compatible with the Euroatom Directives (Euratom Directives,; Summary of the European Directive 2013/59/Euratom (SED), 2015), however local regulations in several aspects of radiological protection are present.

* Corresponding author.
E-mail address: akonefal@us.edu.pl (A. Konefał).

https://doi.org/10.1016/j.radphyschem.2021.109816
Received 3 July 2021; Received in revised form 8 September 2021; Accepted 3 October 2021
Available online 5 October 2021

The procedures associated with the calculation of doses are very important. They are based on national standards which in most cases are compatible with each other as they use NCRP Report 49 (NCRP Report No. 49., 1976). The Polish Norm PN-86 / J-80001 from 1987 is in force in Poland. It is controversial to use the attenuation coefficient *k* included in this standard. This is due to the fact that the *k*-factor values were estimated directly from the transmission curves published in NCRP Report 49 from 1976 based on data obtained in the 1930's, 40's and 50's mainly through simple experiments (Kaye et al., 1936; Braestrup, 1946; Wyckoff and Kennedy, 1949; Kirn et al., 1958; Ritz, 1958; Mooney and Braestrup, 1957; Kennedy et al., 1950; Frantz and Wyckoff, 1959). Some of these data are inconsistent with each other, especially when obtained in independent experiments. An example can be the significantly different transmission curves of gamma rays from ^{226}Ra for the lead shield, presented by Kaye et al. and by Braestrup. At that time, measurements in the field of radiation protection were usually performed without a precise correction of the influence of a detector geometry, beam parameters and other experimental details on results. This problem was highlighted by Wyckoff et al. and Kirn et al., who considered the influence of the position of the detector in relation to the shield on the change of amount of scattered gamma rays reaching the detector and some other aspects connected with scattered radiation. However, at that time many details had to be disregarded due to technological limitations. Unfortunately, the subsequent versions of NCRP Report No. 49 published in 1991, 1994 and 1998 (the last version) contain unchanged transmission curves for isotropic gamma-ray beams. Although in 2005 the NCRP Report No. 151 (NCRP Report No. 151, 2005) was published, which can be considered as the new face of the NCRP Report No. 49, however, it only included new data for therapeutic beams. Problems related to radioactive sources have been omitted in this document. Therefore, values of the attenuation factor *k* covered by the Polish Norm PN-86/J-80001 should be corrected by means of new technologies as the Monte Carlo method realized by computer simulations, which ensures the obtain of high quality results. This work comes out on the point of this challenge. In this study values of the attenuation factor *k* were calculated using the Monte Carlo code - GEANT4 (Agostinelli et al., 2003; Allison et al., 2006; GEANT4) applied commonly in nuclear physics. In this study typical shielding materials were considered. The calculations were performed for the wide range of thicknesses of the shields, including all practical aspects.

In radiological protection in polish institutions it is recommended to estimate the dose in accordance with a strictly defined procedure described in Gostkowska's book (Gostkowska, 2005) based on the mentioned norm. This book is applied by polish radiological protection inspectors for calculation of a dose in workplaces. In this Gostkowska's work values of the gamma-ray attenuation factors *k* in a function of a thickness of the shield are included in charts reprinted from the Polish Norm PN-86/J-80001 and in tables. The additional disadvantage of the factors *k* included in (Gostkowska, 2005) is the lack of compatibility between the *k*-factor values presented in the charts and in the tables. All this does not guarantee accuracy in estimation of a dose, which is required because of risk to exceed the limits of the dose for employees working under conditions of exposure to ionizing radiation.

2. Method

2.1. Determination of the attenuation factor k for isotropic sources of gamma rays

Basic problem related to radiological protection is accurate estimation of a ionizing radiation dose *D* (cGy) in a workplace. For this purpose the commonly used formula is recommended for gamma rays. It can be expressed as follow (Gostkowska, 2005):

$$D = \frac{\Gamma \cdot A \cdot t}{k \cdot l^2}, \tag{1}$$

where Γ (cGy m^2 GBq^{-1} h^{-1}) is the equivalent value of the exposure rate constant, *A* (GBq) – activity of a radiation source, *l* (m) – a distance between a workplace and a location of a gamma - ray isotropic source, *t* (h) – a working time in conditions of exposure to gamma rays and *k* is the attenuation factor for gamma rays. The factor *k* is defined as the ratio of the dose D_0 or dose rate dD_0/dt of incident gamma rays to the dose *D* or dose rate dD/dt of gamma rays transmitted through a shielding material, on the other side of a shield. Thus the attenuation factor *k* can be described in the following way (Gostkowska, 2005):

$$k = \frac{D_0}{D} = \frac{dD_0/dt}{dD/dt}. \tag{2}$$

In this work the factors *k* were determined by means of Monte Carlo simulations for radioisotopes often used in practice in industry, in medicine and in scientific laboratories. The following radioisotopes were considered: ^{60}Co, ^{137}Cs, ^{131}I, ^{192}Ir, ^{198}Au, ^{24}Na, ^{22}Na and ^{59}Fe. The calculations were performed for typical materials used in shielding constructions i.e. concrete (2.3 g/cm^3), lead (11.34 g/cm^3), iron (7.87 g/cm^3) and water (1.0 g/cm^3). The natural composition of elements building the protective materials was introduced into a simulation code. In the simulation of radioactive decays the gamma - ray transitions with emission intensities (*EI*) higher than 0.2% were taken into account. The details are discussed on the example of the ^{59}Fe decay presented in Fig. 1. In the simulation code *EI*'s were represented by the values normalized to 1 for each radionuclide individually. The example with the described approach is presented in Table 1.

In the simulations the upper limits of thicknesses of the shielding material layer were as follow: 120 cm for concrete, 35 cm for iron, 30 cm for lead and 250 cm for water. The considered thicknesses were slightly larger than those included in (Gostkowska, 2005). In this work the Monte Carlo GEANT4 code with the low-energy extension module (also called Livermore) for the simulation of electromagnetic interactions was used. The used module includes models describing the interactions of photons, electrons and positrons with matter down to about 250 eV i.e. close to the K-shell Auger peak from carbon (Journel et al., 2008), using interpolated data tables based on the Livermore library as EADL-EEDL-EPDL (Cullen, EPICS2014). It was validated in many works (Lechner et al., 2010; Cirrone et al., 2010; Kadri et al., 2007), also for complicated geometry (Mesbahi et al., 2005; Konefał et al., 2015). This was a serious argument for using this code in this research.

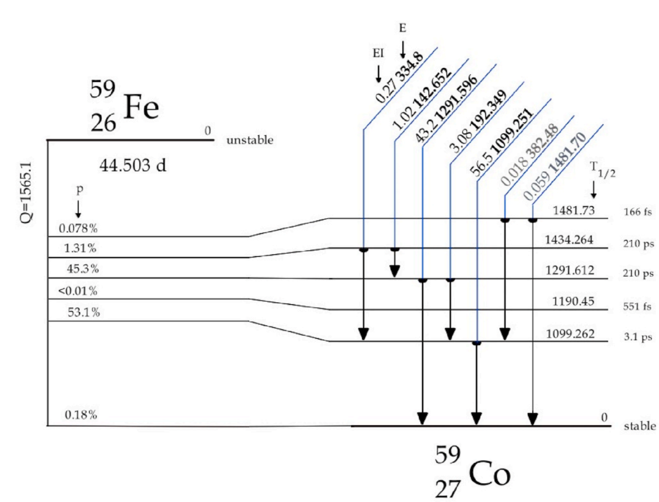

Fig. 1. The scheme of the radioactive decay of the ^{59}Fe radioisotope with the half life of its ground state of 44.503 days; *Q* – energy of the β- decay in keV, *E* – energy of the gamma - ray transition in keV i.e. energy of emitted photons in the gamma decay, *IE* – emission intensity expressed in %, $T_{1/2}$ – a half life of the exited states of the ^{59}Co nucleus, *p* – state occupation probabilities. The transitions with *IE* > 0.2%, were taken into consideration in the simulation.

Table 1
The table contains the chosen data of the gamma ray transitions for the ^{59}Fe radioisotope and parameters used in the simulation code for realizing emission of gamma rays by the ^{59}Fe radiation source. The values of the *wi* parameter define the boundaries of the intervals whose widths are proportional to *EI*. The energy of the emitted photon was determined by the randomly selected value from the w_i parameter range using a random number generator generating a uniform distribution with values in the range <0; 1>. If the randomly selected value was in the range (w_i;w_{i+1}> for $i = 0, \ldots 4$, the emission of a photon with energy E_{i+1} was simulated. This simulation method of gamma decay was applied to all radionuclides considered in this work.

E [keV]	EI [%]	$n_i = EI_i/sum$*	$w_i = \sum_{i=0}^{5} \mathbf{n_i}$**
$E_1 = 142.652$	$EI_1 = 1.02$	$n_1 = 0.0098$	$w_1 = 0.0098$
$E_2 = 192.349$	$EI_2 = 3.06$	$n_2 = 0.0294$	$w_2 = 0.0392$
$E_3 = 334.800$	$EI_3 = 0.27$	$n_3 = 0.0026$	$w_3 = 0.0418$
$E_4 = 1099.251$	$EI_4 = 56.50$	$n_4 = 0.5430$	$w_4 = 0.5848$
$E_5 = 1291.596$	$EI_5 = 43.20$	$n_5 = 0.4152$	$w_5 = 1$

$*\mathbf{sum} = \sum_{i=1}^{5} \mathbf{EI_i} = 104.05$, $**w_0 = 0$.

The geometry of the simulated system consisted of the isotropic point source, the shielding material layer and the 175 cm × 175 cm x 30 cm workplace volume filled with water, corresponding to the space in which the employee may stay at the workplace. A workplace with these sizes represents the volume occupied by the human body when working with gamma ray sources. We assumed a constant distance between the workplace and the radioactive source. We also assumed that an employee may stand upright and, if necessary, move sideways only up to 175 cm (the average height of an adult male) while performing professional activities. The workplace acted as a water logical detector. Water is a material equivalent to biological tissue, recommended by dosimetric protocols for dose determination (IAEA TRS-398, 2006). The use of logical detectors for dose estimation was discussed in (Pietrzak et al., 2016). The dose was recorded in the entire volume of the workplace in order to determine the value of factor *k*. The scheme of the simulated geometry is shown in Fig. 2.

2.2. Verification of the simulation

Verification of the calculation program was carried out by the comparison of results of simulations and measurements for the simple set consisted with a ^{60}Co (or ^{137}Cs) radiation source, a lead shield and a high purity germanium (HPGe) detector placed on the concrete substrate. The experiment was performed using a HPGe detector by Canberra, cooled with liquid nitrogen. In this experiment the lead shields of 30.15 mm, 49.00 mm and 79.15 mm were used. Activities of the used ^{60}Co and ^{137}Cs radiation sources were 0.36 MBq and 2.08 MBq, respectively. The view of the experimental system is presented in Fig. 3. The scheme of the simulated detector is shown in Fig. 4. The simulated geometry mirrored the experimental one. Each measurement lasted 10 min. Values of *k* determined as a relative doses absorbed in the HPGe detector were compared taking into account contributions of photons with energies ranging from 100 keV to 2505.7 keV i.e. to the energy of the ^{60}Co sum peak, when verified by the use of the cobalt source. In the case of verification using the ^{137}Cs source, this energy range was from 100 keV to 661.7 keV. We assumed 100 keV as the low-energy threshold for quantitative verification measurements, because we did not have a professional gamma-ray source that could be used to perform efficiency calibration of the HPGe detector in the range of energies below the adopted threshold. In the low energy range, the qualitative verification was carried out. It consists in comparing the energy spectra from measurements and simulations. The spectra normalized to their maxima were compared.

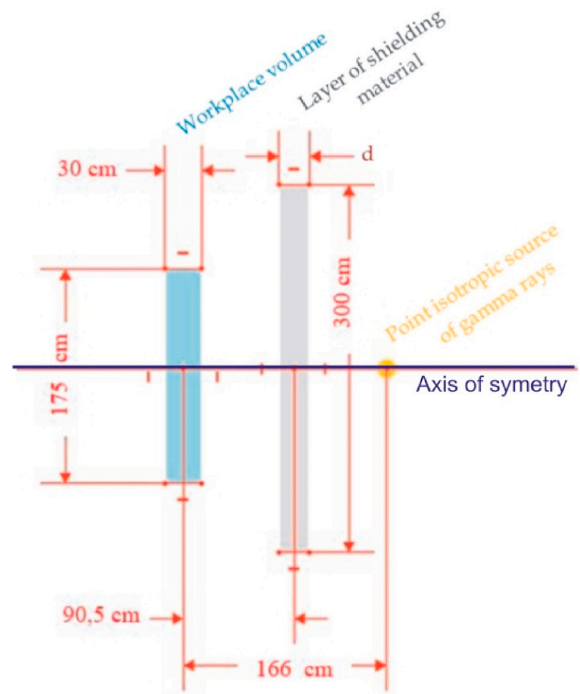

Fig. 2. Scheme of the simulated geometry. *d* – the thickness of the shielding material layer. The upper limits of *d* were given in the text. The simulated system was surrounded by air (0,00129 g/cm^3).

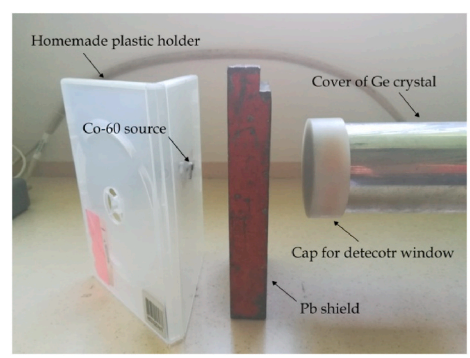

Fig. 3. The ^{60}Co (or ^{137}Cs) source was located in a plastic holder in the axis of the HPGe detector in the distance of 10 cm from the surface of the detector window cap.

3. Results

3.1. Outcomes of verifying study

Results of the calculation program verification are included in Table 2. The experimental errors ΔD_i expressed as a percentage were estimated according to the following formula:

$$\Delta D_i = \frac{\sqrt{N_i}}{N_i} 100\%, \tag{3}$$

where N_i is a number of events registered in the detector, $i = 0$ or $i = d$, where index *i* is equal to 0 for the measurement without the shield and *d* is a thickness of the lead layer. In the verifying experiment the value of the ΔD_i ranged from 0.1% to 0.25% dependently of the thickness of the shield. The final uncertainty of k ($= D_0 / D_d$) can be calculated as follow:

$$\Delta k = \sqrt{(\Delta D_0)^2 + (\Delta D_d)^2}. \tag{4}$$

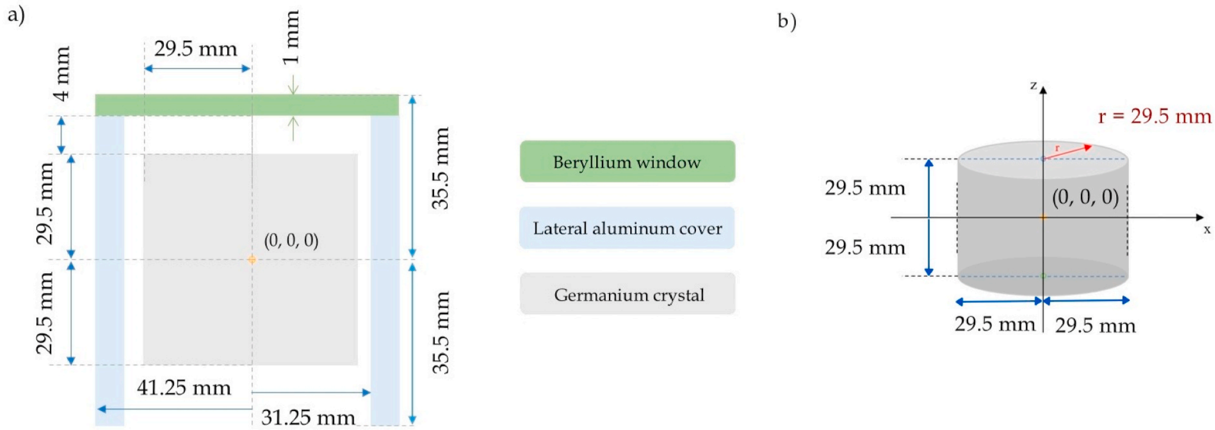

Fig. 4. The scheme of the simulated HPGe detector with sizes of its components. a) The side projection of the detector, b) 3D visualization of cylindrical germanium crystal used in the detector. The center of the germanium crystal is a reference point against which all lengths and distances have been calculated.

Table 2
Summary of the verification of the calculation program.

Thickness d of Pb layer [cm]	k from simulations	k from experiment
a) With the use of the ^{60}Co source.		
3.0	**4**	**4**
4.9	**9**	**8**
7.9	**34**	**36**
a) With the use of the ^{137}Cs source.		
Thickness d of Pb layer [cm]	k from simulations	k from experiment
3.0	**88**	**89**
4.9	**174**	**171**
7.9	**329**	**335**

Δk calculated in this way was 0.3%. The uncertainty Δk determined for the simulations was calculated in the same way as for the experimental values. Regardless of the thickness of the lead shield it did not exceed 0.1%.

The obtained compatibility of the calculated and measured k-factor values is satisfactory. The observed differences are caused by the occurrence of slight density inhomogeneities in the lead layers used in the experiment, what was observed when taking measurements with the same lead bricks symmetrically rotated 180° about the HPGe detector axis passing through the center of the source. Of course, in the simulations homogeneity of the mass distribution in the shielding material was assumed.

Fig. 5 summarizes the spectra for gamma rays from an isotropic ^{137}Cs source after the radiation passed through a 15 cm thick lead layer. In general, the spectra are compatible. The biggest difference is the 7.3 keV Rayleigh scattering peak shift towards higher energies i.e. the experimental peak has its maximum at 186.2 keV, while that of the simulation has its maximum at 193.5 keV.

3.2. Obtained values of the gamma ray attenuation factor k

The results of calculations of the factor k for concrete, lead, water and iron are presented in Fig. 6a–d. The logarithmic scale was used for clear presentation of all subtleties of the characteristics. In the purpose of reduction of statistical fluctuations, the mathematical functions (polynomials, powers and exponentials functions) were fitted using the least squares method to the points obtained from simulations. Additionally, this approach makes the k-factor values continuous distributions in all range of considered thicknesses. It also made it possible to carry out the very sensitive comparison with the values given by Gostkowska in (Gostkowska, 2005). The number of primary gamma rays for each

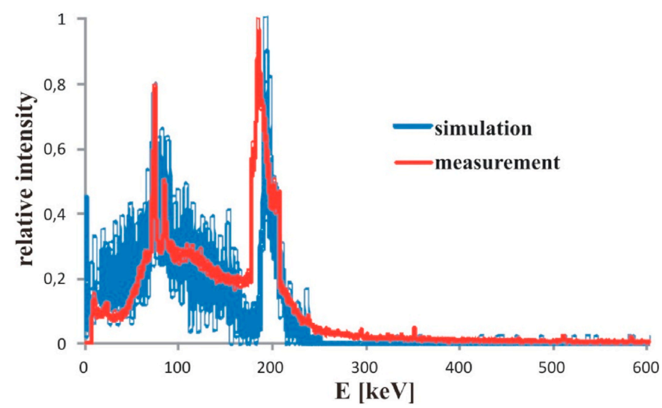

Fig. 5. Comparison of the spectrum obtained from the simulation with the measured spectrum. The spectra were obtained for the isotropic beam of gamma rays from the ^{137}Cs source, immediately after the radiation passed through the 15 cm thick lead shield. The width of the energy bins in which the events were counted in the simulations was 0.4 keV, equal to the energy width of a single channel of the multi-channel analyzer. The adopted width of energy bins enables an accurate comparison of the spectra, however, the simulation spectrum is endowed with large statistical fluctuations.

individual simulation was selected in such a way that maximal statistical fluctuations represented by the difference between the k-factor value estimated with the fixed mathematical function and that taking directly from the simulations does not exceed 1% of the value obtained by simulation. Most often it ranged from 10^7 to 10^9 for a single simulation. All distributions *k(d)* presented in this work were obtained using the described simulation-fit procedure. For the lead shield, the distributions *k (d)* are presented for all eight radioisotopes. For the remaining shielding materials, the distributions *k(d)* of six or seven radioisotopes are shown. Some cases of *k(d)* were omitted in the figures because the k-factor values for ^{59}Fe and ^{22}Na are similar to those for ^{60}Co. Similarly, for water, the k-factor values for ^{198}Au are similar to those for ^{192}Ir and ^{131}I.

The shape of the curves is specific and in most cases the flattening is visible when using a logarithmic scale. For most of these curves the thickness of the layer at which the change of the k-factor gradient is visible i.e. the thickness related to the beginning of the curve flattening area, can be determined. This thickness depends on the type of material and the radionuclide, i.e. the energy of gamma rays. Lower energy of gamma rays and higher material density favor the occurrence of flattening at lower thicknesses of the shield. For example, in the case of ^{198}Au and the lead shield, the flattening of the characteristic becomes noticeable already at 2.5 cm while for ^{60}Co and the iron shield as much

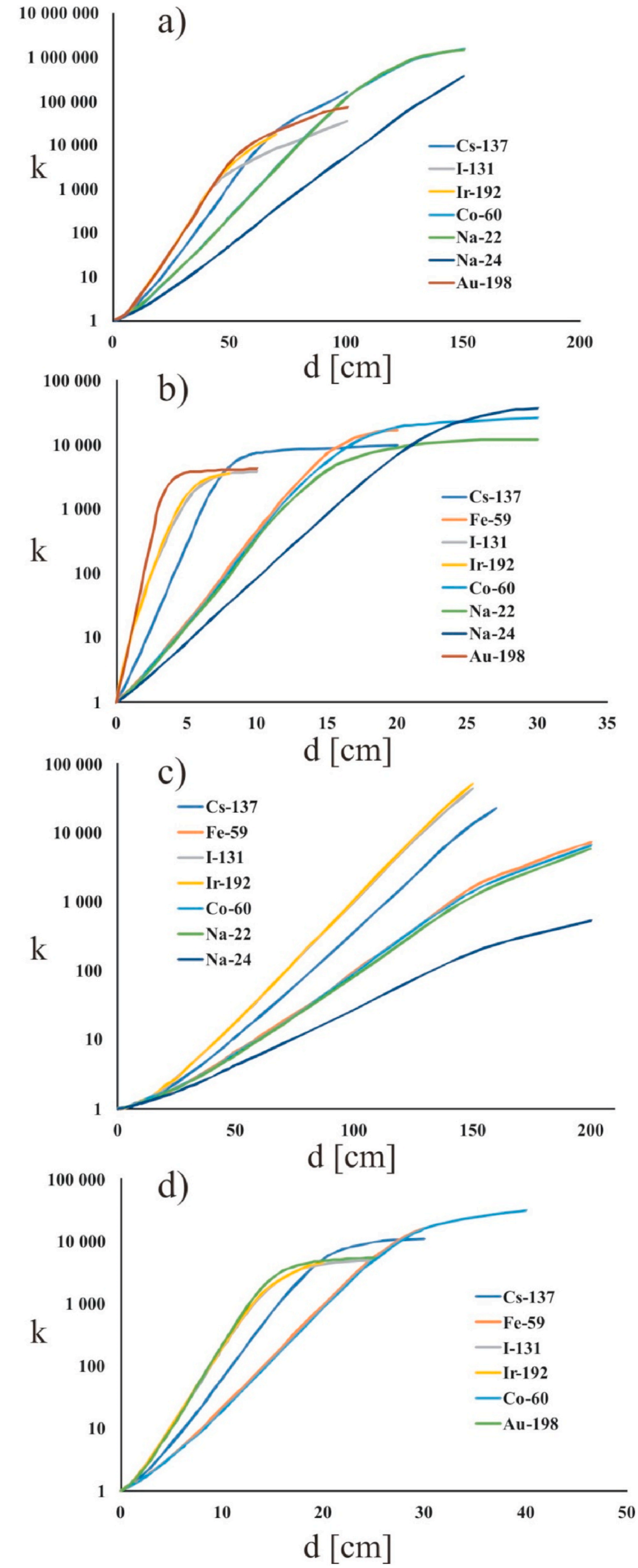

Fig. 6. The gamma-ray attenuation factor *k* versus the thickness *d* of the shield for commonly used shielding materials and radioisotopes. a) concrete, b) lead, c) water and d) iron.

as 29 cm is needed to obtain this flattening. The explanation for this flattening is presented in the next part of the article. The uncertainties of *k* are not shown in the figures showing the dependence *k(d)* because they are not visible in the scale of these figures.

The obtained *k*-factor values were compared with those published by Gostkowska in (Gostkowska, 2005). In the publication by Gostkowska, as mentioned, the values of *k* are presented in charts as well as in tables. However, the data shown in charts differ significantly from those included in tables. Therefore, the separate comparison was made for these two sets of the *k*-factor values (Fig. 7 and Table 3). Fig. 7 shows the comparison of the *k*-factor values for ^{198}Au and lead as a shielding material. In Table 3 the differences between the calculated *k*-factor values and those presented in (Gostkowska, 2005) are included for the chosen thicknesses of the shielding materials for five considered radionuclides.

Additionally, the influence of the size of the volume in which the dose is estimated on the values of *k* was investigated. In these studies, dose calculations were performed for the volume of 175 cm × 175 cm x 30 cm. For comparison, a smaller volume of 5 cm × 5 cm x 5 cm was also considered. The choice of such sizes was not accidental. The smaller volume can be related approximately to the size of the sensitive part of the radiometer containing the Geiger-Müller counters. The larger volume corresponds to the exemplary space in which a person working in conditions of exposure to ionizing radiation can stay at a workplace, as described in the "Methods" section. In the simulations, both volumes were represented by water logical detectors of the above-mentioned sizes. The result of this comparison is presented in Fig. 8.

The *k*-factor values turn out to be dependent on the size of a volume in which a dose is estimated. *k* is larger for the large volume for the same shield thickness. The differences between *k* estimated for the large and the small volume are clearly increasing with the increasing thickness of the shield. They range from a few percent to even 20% for the 30 cm thick lead shield. The difference results from the fact that a larger volume is reached by a greater number of lower-energy photons coming out of the shield at greater angles in relation to the horizontal axis. The water absorption efficiency of these low-energy photons is greater.

The dependence *k(d)* presented in Gostkowska's work is approximately distributed as for a collimated beam, as shown in Fig. 9 for ^{60}Co and the lead shield. The *k(d)* distributions for the collimated beam and for the beam from an isotropic source, calculated using the Monte Carlo method, and the *k*-factor value distributions presented in the chart and the table in (Gostkowska, 2005) were compared. In the case of the *k(d)* distribution for the collimated beam and the distributions presented in Gostkowska's work, there is no flattening typical for isotropic beams.

The attenuation of the collimated photon beam (i.e. the narrow beam) as a result of its passage through a layer of homogeneous matter

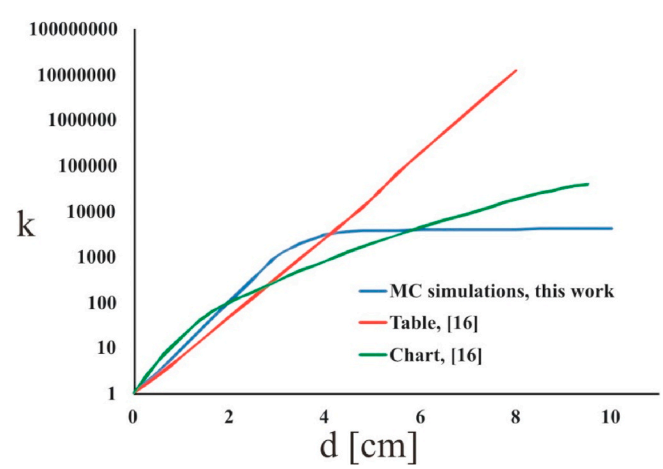

Fig. 7. The gamma-ray attenuation factor *k* determined in this work and that included in (Gostkowska, 2005) versus the thickness *d* of the lead shield for ^{198}Au.

Table 3

The percentage differences between the gamma-ray attenuation factors k estimated in this work and those given by Gostkowska in (Gostkowska, 2005) for the chosen thicknesses of shielding materials. $Diff_{ch} = (k_{tw} - k_{Gc})/k_{tw} \bullet 100$ and $Diff_{tab} = (k_{tw} - k_{Gt})/k_{tw} \bullet 100$, where k_{tw} - the gamma-ray attenuation factor determined in this work, k_{Gc} and k_{Gt} presented in (Gostkowska, 2005), in the charts and in the tables, respectively. The lack of the values in several cells is caused by no data in (Gostkowska, 2005). The negative value of the parameter $Diff_{ch}$ or $Diff_{tab}$ indicates that the value of k determined in this work is less than that delivered by Gostkowska.

Thickness d [cm]	Cs-137		Co-60		Na-24		Au-198		I-131	
	$Diff_{tab}$	$Diff_{ch}$	$Diff_{tab}$	$Diff_{ch}$	$Diff_{tab}$	$Diff_{ch}$	$Diff_{tab}$	$Diff_{ch}$	$Diff_{tab}$	$Diff_{ch}$
	Concrete									
10	31.6	15.4	21.5	1.8	16.6	16,9	52,5	−67,6	44,1	−14,6
50	82,6	53,6	74,0	58,1	56,3	60,6	73,8	27,6	7,6	80,7
100	−64,1	x	88,0	77,4	64,1	78,2	−6418,6	X	−19010.3	x
	Lead									
1	6,5	−13,7	9,7	3,3	8,4	−6,2	33,2	−76,8	18,5	17.0
5	30.5	26.9	10.8	13.5	15.6	1.1	−396.9	46.7	−5188.7	23.2
10	−784.3	−565.2	36.4	19.8	34.8	16.5	X	X	x	x
	Water									
10	21.2	13.3	21.0	21.0	18.4	2.1	22.6	22.6	22.5	22.5
50	40.1	59.1	16.9	37.8	14.8	18.1	52.1	58.0	56.7	55.9
100	60.9	56.1	44.0	37.7	18.8	26.7	68.0	55.8	56.2	56.0
	Iron									
5	18.2	−25.0	10.8	−1.1	X	x	19.0	28.6	14.1	16.7
10	37.5	26.6	26.7	−3.7	X	x	45.0	42.9	28.5	49.5
20	12.0	38.4	50.0	38.0	X	x	−1142.0	X	−2232.7	x

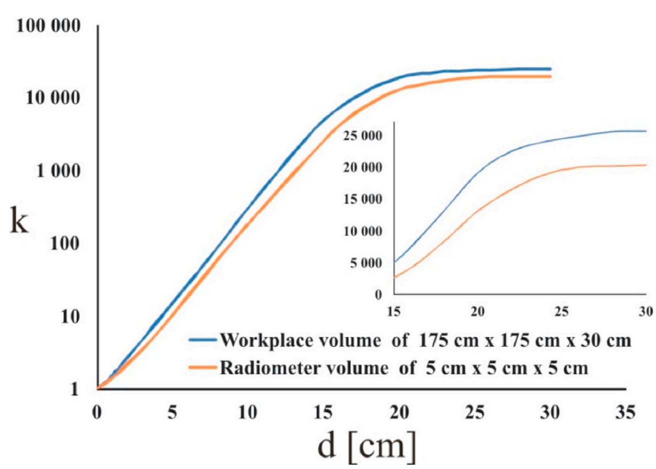

Fig. 8. The k-factor value distributions for workplaces of various sizes. The blue line represents the workplace of 175 cm × 175 cm × 30 cm whereas the red one shows the distribution for the 5 cm × 5 cm × 5 cm volume of a radiometer. The presented curves were derived for ^{60}Co and the lead shield. The zoom of the area between 15 cm and 30 cm is shown with no logarithmic scale in the inset. (For interpretation of the references to colour in this figure legend, the reader is referred to the Web version of this article.)

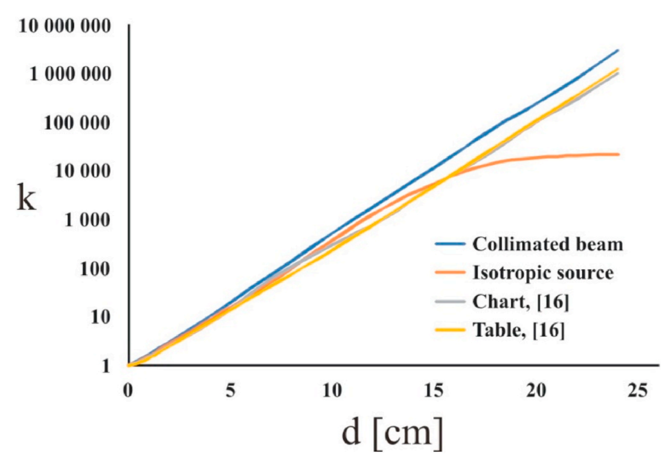

Fig. 9. The comparison of the k-factor values calculated using the Monte Carlo method for the isotropic source and the collimated beam, for Co-60, with those presented in the chart and in the table in (Gostkowska, 2005).

can be defined by the following formula:

$$k = e^{\mu d}, \tag{5}$$

where μ (cm^{-1}) is the photon linear attenuation coefficient. In Fig. 10 the dependence 5) was fitted to the data from (Gostkowska, 2005) and from this work.

The distributions *k(d)* presented by Gostkowska can be precisely described by the relation 5) typical for narrow (collimated) beams of photons, not suitable for isotropic sources of gamma rays while the data obtained in this work clearly differ from this dependence. This proves that the transmission curves contained in NCRP Report No. 49 being the main base for the Polish Norm PN-86/J-80001, were most likely derived by the extrapolation method using the function contained in formula 5), of course appropriately transformed to the description of the transmission curves i.e:

$$T = k^{-1} = e^{-\mu d}, \qquad 6)$$

where T is a transmission coefficient. Thus, the k-factor values, and thus also the transmission curves from the NCRP Report No. 49, require correction so that they could be used for beams from isotropic gamma-ray sources. It is true that this NCRP document also includes transmission curves for scattered gamma rays. However, these curves also show no distribution properties for isotropic sources. Additionally, NARP Report No. 49 does not include data for water as a shielding material.

The *k(d)* curves for isotropic beams in the range of smaller thicknesses of a shield run over the distributions for narrow beams. For example, for the ^{198}Au source up to a lead thickness of 4 cm, the obtained k-factor values are greater than those presented in the tables in (Gostkowska, 2005) (Fig. 7). Similarly for ^{60}Co, this area appears in the range of lead shield thicknesses up to 15 cm (Fig. 9). It is due to the fact that in the case of an isotropic beam the path of the photons in the shielding material is longer than in the case of narrow beams, and thus the energy degradation of the isotropic beams is greater. This degradation of energy is mainly a consequence of Compton scattering. This leads to a stronger absorption of the isotropic beam, which gives k-factor values being greater for the isotropic beam than for the narrow beam. This tendency is broken when there is a flattening in the *k(d)* distribution for isotropic beams. This flattening not observed with a narrow

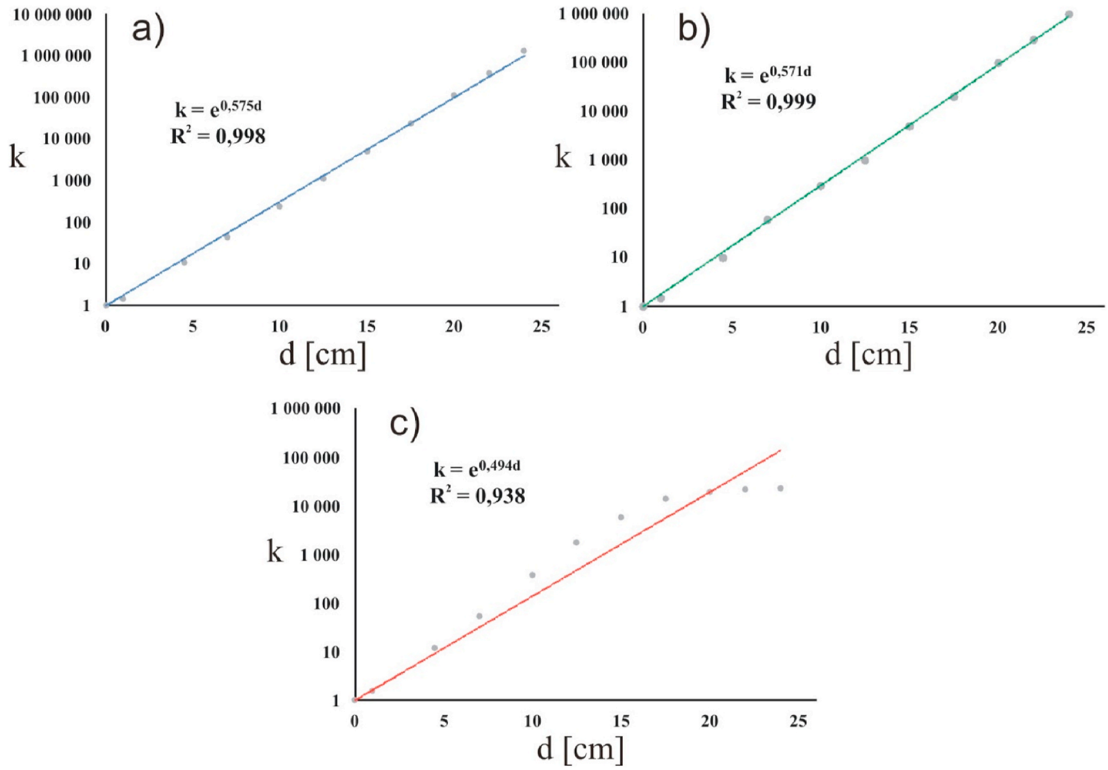

Fig. 10. The results of fitting of the exponential function to the data read from (Gostkowska, 2005), using the least squares method, a) the data from the table and b) from the chart for ^{60}Co and lead. The analogous fitting procedure was applied to the dependence *k(d)* determined in this work c). A value of the square of the Pearson coefficient R^2 close to 1 indicates that the fitted function describes the distribution *k(d)* very well.

beam is primarily caused by low-energy photons causing a difference in the quality of gamma rays reaching the workplace. This fact is illustrated by the spectra of the energy absorbed in the workplace, presented in Fig. 11, for a collimated and isotropic ^{60}Co beams, for two lead shield thicknesses of 15 cm and 20 cm.

The low-energy photons giving the first peak in the spectrum for the isotropic beam come from incoherent Compton scattering on electrons of lead atoms, which causes energy degradation of these photons and Doppler broadening of their energy distribution. Doppler broadening results from the pre-collision motion of the bound electrons. Of course, due to the strong photoelectric effect absorption in the lead in the energy range of these photons, those that reach the logical detector are mostly formed in the part of the shield closest to the workplace. In addition, the spectrum for the isotropic source shows a peak at about 200–220 keV. It corresponds to the energy of the photons that leave the lead shield due to Rayleigh scattering. It is at about 200–220 keV that the Rayleigh cross section becomes comparable to the Compton and photoelectric cross sections, which allows many photons to avoid another incoherent scattering, as well as their complete absorption by the electron shell of lead atoms. However, in the case of the collimated beam spectrum, the dominance of primary and other higher-energy photons is visible. This results in much lower energy absorbed in the workplace for the 20 cm thick shield compared to absorption for the 15 cm thick one. Quantitative analysis of the spectra showed that the energy absorbed in the workplace for the shield of 20 cm is only 4.9% of the energy absorbed for the 15 cm shield. In the case of an isotropic beam, this fraction of the absorbed energy is much larger, it amounts to 18.3%, and this is mainly due to the absorption of low-energy photons with energies below 100 keV. Additionally, the higher energy absorption efficiency for the beam from isotropic sources results from the fact that isotropically emitted photons fall on the workplace surface at different angles and therefore they can travel greater distances in the logical detector, giving the water more energy, while the photons of the collimated beam move along trajectories close to the beam axis and thus their trajectories in the water will be shorter and less energy left. The explanation of this phenomenon is presented in Fig. 12 showing the energy absorption efficiency curves $\varepsilon_{ab}(E)$ for the applied workplace for two beams with photon trajectories creating angles of 0° and 30° with the axis of symmetry of the simulated system.

It is worth noting that the flattening of the *k(d)* curves characterized by a small *k*-factor gradient occurs in a relatively large range of shield thicknesses. The reason for the low gradient is relatively a small change in the quality of the isotropic beam of photons reaching the workplace, manifested by a small change in the energy spectrum of these photons in the range of shield thicknesses where this flattening is observed. This is evidenced by the comparison of the spectra of the photon energy absorbed in the logical detector for the isotropic ^{137}Cs source and the lead shield with a thickness of 10 cm and 20 cm (Fig. 13a).

As for lead, one can explain the flattening of *k(d)* curves for other shielding materials. Fig. 13b shows the spectra of the photon energy absorbed in the logical detector after the isotropic beam of photons from the ^{137}Cs source has passed through the iron layers with a thickness of 20 cm and 24 cm. For iron, two peaks are also visible.

4. Discussion

Application of the Monte Carlo simulation makes it possible to get the high quality results even for the thick shields. The disadvantage of the experimental approach is necessity of the application of radiation sources with high activity, particularly for thicker shielding layers which is connected with the increased radiation risk. This problem disappear when the experiment is replaced by simulations. Additionally, the use of logical detectors permits to avoid the perturbation of the radiation fluence caused by a detector affecting a measurement result.

As mentioned, the gamma-ray attenuation factors *k* given in (Gostkowska, 2005), are presented in charts as well as in tables. However,

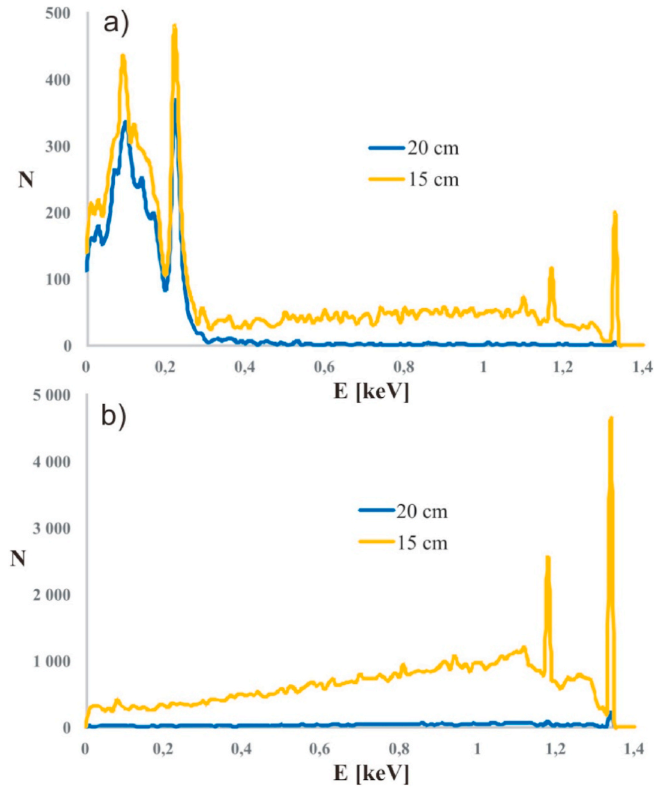

Fig. 11. The energy spectrum of photons reaching the 175 cm × 175 cm x 30 cm water workplace (logical detector), using the ^{60}Co source and the lead shield, a) for the isotropic beam, b) for the collimated beam, for two chosen thicknesses of the lead shield of 15 cm and 20 cm. These shield thicknesses were chosen for this comparison, because for the 15 cm shield the *k*-factor values for both beam types are similar, while for the 20 cm shield there is a large discrepancy between the *k(d)* distributions. *N* – the number of events registered in the 10 keV bin per 2•10^8 primary photons, *E* – energy of photons registered in the logical detector.

values of *k* from the charts differ from those included in the tables even about two hundred percent. The differences are much higher than uncertainties caused by the readout from the charts. Additionally, the *k*-factor values presented in (Gostkowska, 2005) and in the Polish Norm PN-86/J-80001 are largely based on NCRP Report No. 49 and therefore on experiments from 1930's, 40's and 50's. In that time any investigations were not supported by the Monte Carlo method or another precise calculation method. This points to the need to determine the *k*-factors using modern technologies.

It is also worth noting that in (Gostkowska, 2005) the mean energies of gamma rays from decays are strongly approximate. For example, the energy suggested by Gostkowska for calculations for ^{192}Ir is 0.6 MeV whereas this energy is equal to 371.9 keV when calculating accurately according to the radioactive decay, taking into account all transitions with emission intensity (*EI*) greater than 0.2%. Precision in estimation of gamma-ray mean energy affects to a choice of the *k*-factor value for a dose calculation when estimated with the use of the tables included in the Gostkowska's book. All this makes that the dose estimated using values of *k*-factor from (Gostkowska, 2005) is not reliable. The use of the data from Gostkowska's work can involve the error impossible to estimate. This study provides the comprehensive data with the possibility of distribution of the electronic version. Furthermore, this work is the unification of approach for the *k*-factor value determination.

The applied GEANT4 code provides the possibility to simulate such subtle processes as the Compton scattering of low-energy photons on the electrons of an atom, taking into account the Doppler effect. The atomic shell effects in the Compton scattering are included in the G4KleinNishinaModel used in the simulation program in this work. In this model the angular and energy distribution of the incoherently scattered photon is given by the product of the differential Klein-Nishina formula and the so-called incoherent scattering function studied by Hubbell (Hubbell et al., 1974). Several other scientific codes also provide the ability to simulate the described effects. An example would be the code EGS4 (Nelson et al., 1985).

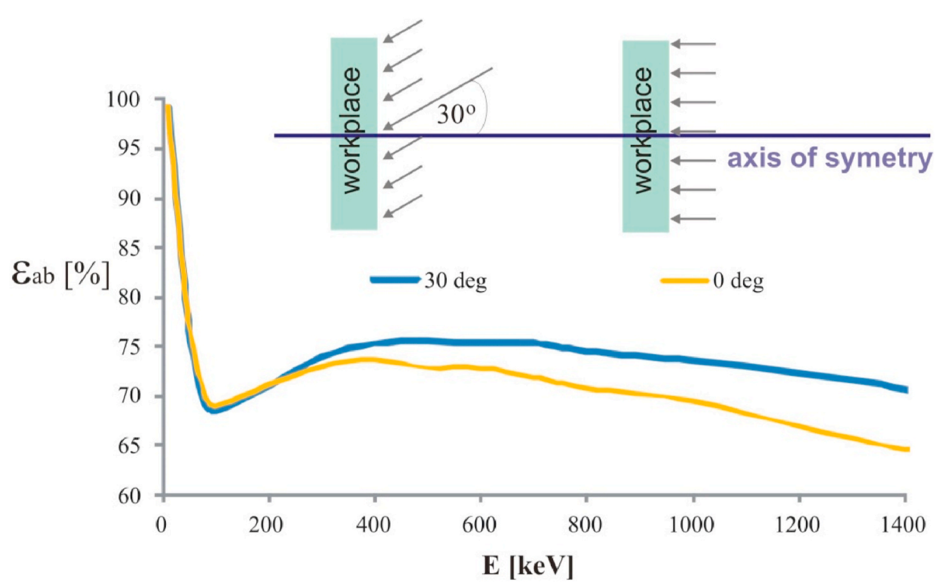

Fig. 12. The absorption efficiency curves versus the photon energy – $\varepsilon_{ab}(E)$ for photons absorbed in the 175 cm × 175 cm x 30 cm water workplace (logical detector), for photons whose trajectory directions create angles of 0 and 30° with the axis of symmetry of the system. The photon movement directions at the place of entry to the workplace are marked with arrows.

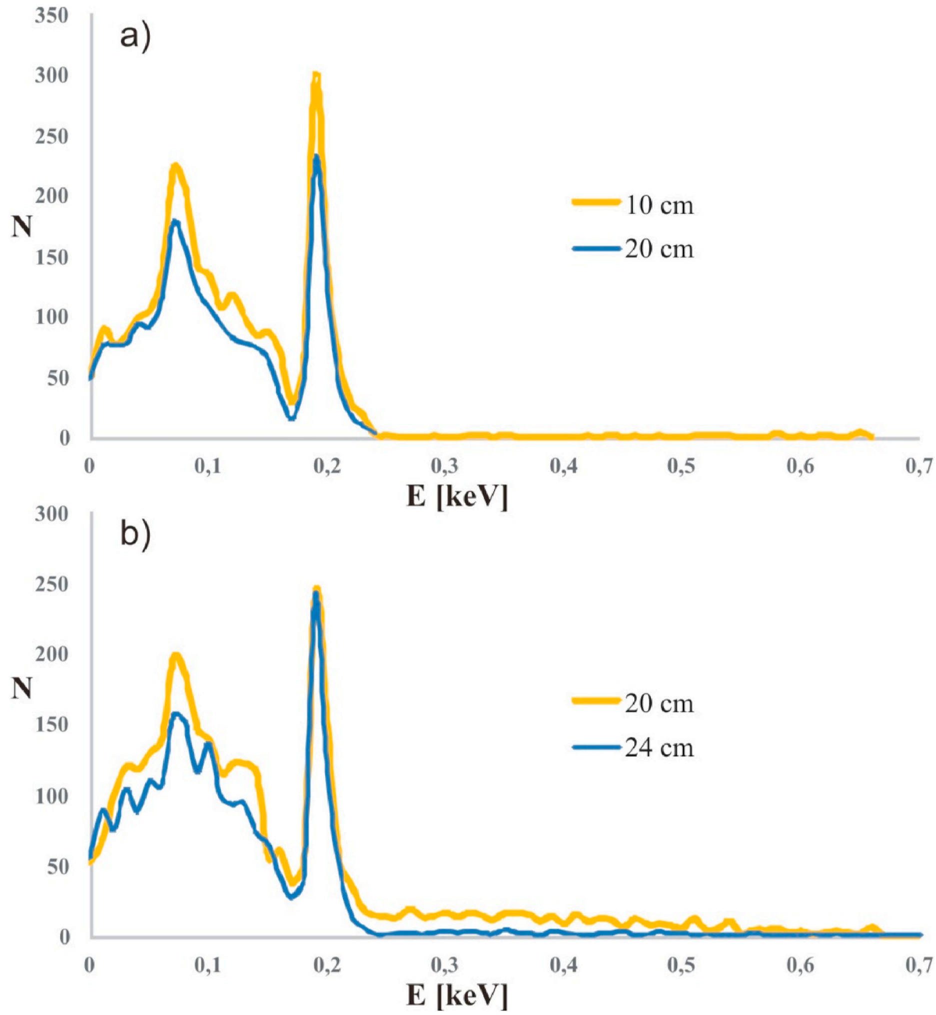

Fig. 13. The spectra of the photon energy absorbed in the workplace (logical detector) for gamma rays from the isotropic ^{137}Cs source passing through a) the 15 cm and 20 cm thick lead shield and b) the 20 cm and 24 cm thick iron one, i.e. within the range of the flattening of the *k(d)* curve. The spectra presented in Fig. 13a were obtained for $2 \cdot 10^8$ primary photons whereas these in Fig. 13b for 10^8 ones. Otherwise as in Fig. 11.

5. Conclusions

This work provided very accurate values of the gamma-ray attenuation factor *k* for the commonly used isotropic gamma-ray sources and typical protective materials. Application of the Monte Carlo method made it possible to get accurate data in the wide range of the shield thicknesses without the use of strong radiation sources and the extrapolation method. In spite of the fact that the main motivation of this work was improvement of the dose estimation procedure used in radiological protection in Poland, the obtained *k*-factor values have universal character and they can be applied in all procedures of a dose calculation when the gamma-ray attenuation factor *k* appears.

The gamma-ray attenuation factors *k* included in the Gostkowska's book and in the Polish Norm PN-86/J-80001 as well as the transmission curves presented in the NCRP Report No. 49 and in the subsequent versions of this document published in 1991, 1994 and 1998 (the last version) have no practical significance because they do not induce the effects related to the isotropic gamma-ray sources. Therefore, their use can lead to serious errors in dose estimation in the workplace and furthermore leads to a large underestimation of the dose when using thicker shields. As mentioned, in 2005 the NCRP Report No. 151 was published, which can be considered a new face of the NCRP Report No. 49. However, it only includes new data for therapeutic beams. Problems related to radioactive sources have been omitted in this document. Therefore this presented work is important for ensuring high-quality dose estimation in radiation protection also in industry and in scientific laboratories. Obviously, the *k*-factors determined in this study are related to the applied geometry of the simulated system including the radioactive source, the shield and the workplace. Any change in the workplace size, the source-shield distance, etc. will affect the *k*-factor values. The greater these changes, the more pronounced these impact will be. Research on the influence of geometry on the *k*-factor values will be the purpose of our further investigations.

It is worth noting that in recent years, the novel materials have appeared and are used as the shields, since traditional radiation shielding materials, namely lead and concretes, have few disadvantages such as toxicity, strength, etc. Many researchers reported some novel and alternative shielding materials such as glass or polymer to prevent from gamma radiation (Agar et al., 2019; Kaur et al., 2017). The modern γ-ray shields are often made from some binary alloys: Pb–Sn, Pb–Zn, and Zn–Sn, or from the multiple elements. The lower atomic number component present in the alloy may prove to be an effective filter for low-energy photons due to the much larger cross-section for absorption by the photoelectric effect, compared to the Raleigh scattering cross section at lower energies. However, this requires detailed research.

Author statement

Marta Błażkiewicz - Data curation; Formal analysis; Investigation; Supervision; Validation; Resources; Visualization; Roles/Writing –

original draft.

Adam Konefał – Conceptualization; Data curation; Formal analysis; Methodology; Software; Project administration; Resources; Visualization; Roles/Writing – original draft; Writing – review & editing.

Declaration of competing interest

The authors declare that they have no known competing financial interests or personal relationships that could have appeared to influence the work reported in this paper.

References

Agar, O., et al., 2019. An extensive investigation on gamma ray shielding features of Pd/Ag-based alloys. Nucl. Engin.Technol. 51, 853–859.

Agostinelli, S., et al., 2003. GEANT4 - a simulation toolkit. Nucl. Instrum. Methods Phys. Res. A 506, 250–303.

Allison, J., et al., 2006. GEANT4 developments and applications. Nucl. Instrum. Methods Phys. Res. A 835, 186–225.

Braestrup, C.B., 1946. Protection measurements of lead - shielded radium. Radiology 46, 385–390.

Cirrone, G.A.P., et al., 2010. Validation of the Geant4 electromagnetic photon cross-sections for elements and compounds. Nucl. Instrum. Methods Phys. Res. A 618, 315–322.

Cullen, D.E., 2015. EPICS2014: Electron Photon Interaction Cross Sections. Documentation Series of the IAEA Nuclear Data Section.

Euratom Directives. http://www.ensreg.eu/nuclear-safety-regulation/eu-instruments/Basic-Safety-Standards-Directive.

Frantz, F.S., Wyckoff, H.O., 1959. Attenuation of scattered cesium-137 gamma rays. Radiology 73, 263–266.

Gostkowska, B., 2005. Radiological Protection. Quantities, Units and Calculations. The Central Laboratory for Radiation Protection, Warsaw.

Hubbell, J.H., Veigele, W.J., Briggs, E.A., Brown, R.T., Cromer, D.T., Howerton, R.J., 1974. Atomic form factors, incoherent scattering functions, and photon scattering cross sections. J. Phys. Chem. Ref. Data 4, 471–616.

IAEA TRS-398, 2006. Absorbed Dose Determination in External Beam Radiotherapy: an International Code of Practice for Dosimetry Based on Standards of Absorbed Dose to Water. International Atomic Energy Agency, Vienna.

Journel, L., Guillemin, R., Haouas, A., Lablanquie, P., Penent, F., Palaudoux, J., Andric, L., Simon, M., 2008. Resonant double Auger decay in carbon K-shell excitation of CO. Phys. Rev. 77, 042710.

Kadri, O., Ivanchenko, V.N., Gharbi, F., Trabelsi, A., 2007. GEANT4 simulation of electron energy deposition in extended media. Nucl. Instrum. Methods Phys. Res. B 258, 381–387.

Kaur, T., Sharma, J., Singh, T., 2017. Thickness optimization of Sn-Pb alloys for experimentally measuring mass attenuation coefficients Nucl. Energy Technol. 3, 1–5.

Kaye, G.W.C., Bell, G.E., Binks, W., 1936. The protection of radium workers from gamma radiation. Br. J. Radiol. 9, 161–171.

Kennedy, R.J., Wyckoff, H.O., Snyder, W.A., 1950. Concrete as a protective barrier for gamma-rays from Cobalt-60. J. Res. Natn. Bur. Stand. 44, 157–162.

Kirn, F.S., Kennedy, R.J., Wyckopf, H.0., 1958. Attenuation of gamma rays at oblique incidence. Radiology 63, 94–104.

Konefał, A., Bakoniak, M., Orlef, A., Maniakowski, Z., Szewczuk, M., 2015. Energy spectra in water for the 6 MV X-ray therapeutic beam generated by Clinac-2300 linac. Radiat. Meas. 72, 12–22.

Lechner, A., Ivanchenko, V.N., Knobloch, J., 2010. Validation of recent Geant4 physics models for application in carbon ion therapy. Nucl. Instrum. Methods B 268, 2343–2354.

Mesbahi, A., Fix, M., Allahverdi, M., Grein, E., Garaati, H., 2005. Monte Carlo calculation of Varian 2300C/D Linac photon beam characteristics: a comparison between MCNP4C, GEANT4 and measurements. Appl. Radiat. Isot. 62, 469–477.

Mooney, R.T., Braestrup, C.B., 1957. Attenuation of Scattered Cobalt-60 Radiation in Lead and Building Materials. AEC Report NYO 2165.

NCRP Report No. 151, 2005. Structural Shielding Design and Evaluation for Megavoltage X- and Gamma-Ray Radiotherapy Facilities. Bethesda.

NCRP Report No. 49., 1976. Medical X-Ray and Gamma-Ray Protection for Energies up to 10 MeV. Structural Shielding Design and Evaluation. Washington.

Nelson, W.R., Hirayama, H., Rogers, D.W.O., 1985. The EGS4 Code System. SLAC-265.

Pietrzak, R., Konefał, A., Sokół, M., Orlef, A., 2016. Comparison of depth-dose distributions of proton therapeutic beams calculated by means of logical detectors and ionization chamber modeled in Monte Carlo codes. Nucl. Instrum. Methods Phys. Res. A 826, 55–59.

Polish Nuclear Law, 2003. http://www.ilo.org/dyn/natlex/natlex4.detail?p_lang=en&p_isn=68307. (Accessed 29 November 2000) accessed.

Ritz, V.H., 1958. Broad and narrow beam attenuation of Ir^{192} gamma rays in concrete, steel and lead. Non-Destr. Test. 16, 269–272.

Summary of the European Directive 2013/59/Euratom, 2015. Essentials for health professionals in radiology. Insights Imaging 6, 411–417. https://doi.org/10.1007/s13244-015-0410-4.

The web site of the GEANT4 project (GEANT4). https://geant4.web.cern.ch/node/1.

Wyckoff, H.O., Kennedy, R.J., 1949. Concrete as a protective barrier for gamma rays from radium. J. Research NBS 42, 431–435.